COBEM 2021 26th International Congress of Mechanical Engineering
November 22-26, 2021, Virtual Congress, Brazil
ABCM Associação Brasileira de Engenharia e Ciências Mecânicas

COBEM2021-0147
A COMPARATIVE STUDY OF THERMAL ERRORS OF 5-AXIS MACHINING CENTERS OBTAINED USING THE LASER INTERFEROMETER DEVICE USING THE EXPERIMENTAL AND NUMERICAL METHODS

Marcelo Otávio dos Santos
Éd Claudio Bordinassi
Adalto de Farias
Instituto Mauá de Tecnologia, Praça Mauá, 01 – São Caetano do Sul/SP – 09580-900
FEI - Centro Universitário da Fundação Educacional Padre Saboia de Medeiros – Av. Humberto de Alencar Castelo Branco, 3972, S. Bernardo do Campo/SP – 09850-901
marcelo.santos@maua.br / mosantos@fei.edu.br
ecb@maua.br / edbordinassi@fei.edu.br
adalto.farias@maua.br / afarias@fei.edu.br

Rodrigo Lima Stoeterau
Gilmar Ferreira Batalha
Escola Politécnica da Universidade de São Paulo - Av. Prof. Luciano Gualberto, 380 – São Paulo/SP - 05508-010
rodrigo.stoeterau@usp.br
gfbatalh@usp.br

Abstract. *This work aimed to measure and compare the thermal errors obtained in the linear axes X, Y and Z of a 5-axis universal machining center, by the experimental and numerical methods. The experimental data were obtained by an interferometer laser device measurements after carrying out heating cycles of the machine. The numerical results were obtained through the finite element modeling, simulating the heating cycles in the machine and collecting the thermal errors in the same stop positions that were considered in the experimental stage. For the experimental thermal monitoring, 15 temperature sensors were installed at critical points on the machine. The measurements of thermal errors were divided into two stages. In the first stage, measurements were made in the condition of a "cold machine". This step was intended to map the initial positioning errors of the machine. In the second stage, measurements were made after running a 4-hour heating cycle. In the thermoelastic analysis by finite elements, the same operational and environmental conditions in which the machining center was exposed during the experimental stage were depicted. For the three axes analyzed, the results were quite satisfactory, with the differences between the experimentally measured and simulated errors being less than 7.5 µm for the X axis, less than 9.6 µm for the Y axis and less than 2.5 µm for the Z axis.*

Keywords: *Thermal error, 5-axis machining center, interferometer laser device, finite elements method.*

1. INTRODUCTION

In the 21st century, the metal mechanic industry and Industry 4.0 are continually growing together and these new possibilities open the way for making machines more accurate and reliable. There are several errors that interfere in the machining processes. The thermal error seriously hinders enhancing of machine tool's thermal stability (Liu *et al*., 2021) and machining error related to thermal effects is approximately 50-70% (Miao *et al*., 2015 and Jedrzejewski, *et al*., 2008). When the machine tool is in operation, thermal deformation is inevitable, as the temperature related to the movement of machine parts is dynamically affecting the entire process (Zhou *et al*., 2018). Generally, the temperature of the machine is affected mainly by following factors, the internal heat generated by the work of the machine's motors, friction in bearings, ball screw etc. (Abdulshahed *et al*., 2015) and those caused by the machine tool cutting process, that then causes thermal elastic deformation resulting in the geometric and shape errors of machined workpieces (Liu *et al*., 2017). Another factor is the ambient influence through radiation and thermal convection between the machine and the outside where the machine is located (Zhou *et al*., 2018).

For the study of thermal errors, it is necessary to analyze some important points. To reduce or eliminate machine tool errors, many attempts and great efforts have been made during the last decades. Some manufacturers are able to achieve high accuracy by improving design methodologies and advancing materials technologies. It is much easier to monitor or measure the amount of inaccuracies and compensate through changes in the commanded position of different axes, which is especially applicable to CNC machine tools (Zhao *et al*., 2017 and Gurauskis *et al*., 2019). Monitoring is necessary

because users have realized that machines that are similar in performance and course of work, for example, can present significantly different thermal errors (Mayr *et al*., 2012). Another way to reduce the resulting error induced by the thermal expansion of the machine tool is to heat the machine tool before the actual cutting process. When the machine tool's thermal equilibrium state is reached, the machine tool can be used for the actual cutting of parts. The heating process is usually time-consuming, often takes hours, which affects the overall efficiency of machining manufacturing and is not ecological (Zhang and Wu, 2019). According to Miao *et al*. (2015), the selection of temperature-sensitive points, which have the most important influence on thermal error, is based on selecting the smallest number of temperature sensors to obtain the best fit and prediction effects and robustness for a thermal error model.

In the last years, there has been a significant advance in technologies aimed at monitoring and Industry 4.0, and their use has increased knowledge about the origin of thermal errors (Drossel *et al*., 2013). This concept presents a new generation of smarter, better connected, widely accessible, more adaptive and more autonomous machine tools (Liu *et al*., 2018).

This work aims to measure and compare the thermal errors of the three linear axes of a 5-axis universal machining center through laser interferometer measurement and then perform the finite element modeling of this process by comparing the results obtained by the simulations with the results obtained experimentally. The main contribution of this work will be able to play the same thermal errors obtained by the real operation of the machine through computer simulation using appropriate thermal and mechanical boundary conditions.

2. METHODS AND MATERIALS

2.1 Equipments

The machine tool used to carry out the experimental research of thermal errors was a 5-axis GROB universal machining center, model G550AB (Figure 1) with positioning tolerance of 6 µm.

Figure 1. Machining center G550AB installed in the technology center of B. GROB of Brazil company.

The interferometer laser encoder used to measure the thermal errors of the linear axes X, Y and Z of the machining center is type XL-80 from the manufacturer RENISHAW, with linear resolution of 1 nm and measurement accuracy of ±0.5 ppm, as Figure 2. Laser interferometry is a well-established method for measuring distances with great accuracy and is widely used for machine tool evaluation due to its versatility.

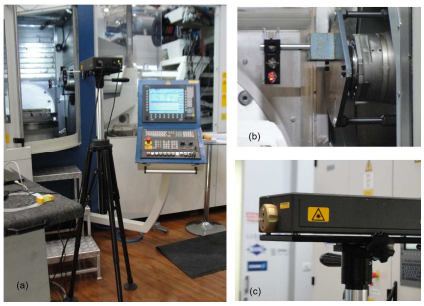

Figure 2. Laser interferometer encoder (a) tripod for laser gun with mounted retro-reflectors, (b) retro-reflector mounted at the spindle tip, (c) laser head.

For the thermal monitoring of the machining center, 15 thermocouple-type temperature sensors were installed at critical points on the machine, which continuously measured and recorded the temperature variation every 5 minutes. Figure 3 shows the locations where the temperature sensors were installed in the machining center.

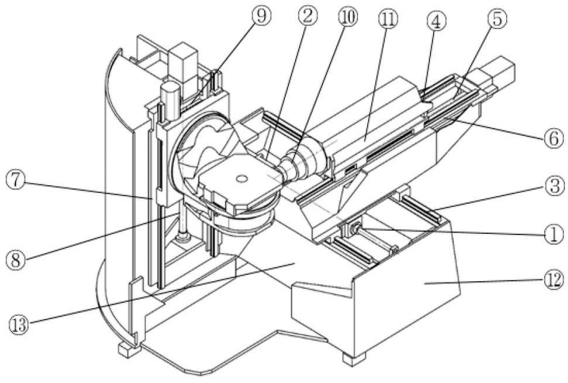

Figure 3. Installation locations of temperature sensors on the machine.

Table 1 shows the locations where the 15 temperature sensors used for thermal monitoring of the machining center were installed.

Table 1. Installation locations of temperature sensors.

Sensor code	Sensor installation locations
T1	Ball Screw Nut (X axis)
T2	Motor bearing (X axis)
T3	Linear guide (X axis)
T4	Ball Screw Nut (Z axis)
T5	Motor bearing (Z axis)
T6	Linear guide (Z axis)
T7	Ball Screw Nut (Y axis)
T8	Column inner wall (Y axis)
T9	Motor bearing (Y axis)
T10	Motor spindle tip (Z axis)
T11	Motor spindle outer casing (Z axis)
T12	Machine base
T13	Working area base
T14	Coolant tank
T15	Room temperature

2.2 Experimental procedure

Positioning error measurements were divided into two steps. In the first stage, measurements were carried out in the "cold" machine condition, that is, the machining center had a temperature in equilibrium with the environment at 20°C. This step was intended to map the machine's initial positioning errors.

In the second stage, measurements were taken after running the warm-up cycle, ensuring through temperature monitoring a "heated" machine condition, that is, at the temperature obtained at the end of the warm-up cycle (Table 2). In this way, it was possible to evaluate the thermal error of positioning of the linear axes X, Y and Z of the machining center. During the warm-up cycle, the five axes of the machining center were activated simultaneously and the objective was to evaluate the thermoelastic behavior of the machine during a slightly higher than usual working condition.

Table 2. Machining center warm-up cycle.

Warm-up Cycle	X-axis speed	Y-axis speed	Z-axis speed	Spindle speed	A-axis speed	B-axis speed
	30 m/min	30 m/min	30 m/min	12,000 rpm	8 rpm	30 rpm
Duration	X-axis travel	Y-axis travel	Z-axis travel	----	A-axis travel	B-axis travel
4 hours	800 mm	950 mm	1,020 mm	----	240°	360°

2.3 Numerical simulation of laser thermal error measurement

The finite element numerical simulation (FEA) was performed for the complete machine, where the feed units of the X, Y and Z axes were offset, which will allow the evaluation of the thermal influence for different positions of the axes as verified experimentally by reading the laser interferometer.

In the FEA model of the machine, 412,786 tetrahedral elements of second order were used, totaling 747,397 nodes with element size of 50 mm in the machine structure, 40 mm in the work table and 25 mm in the sliding units (Figure 4a) which guaranteed an average aspect ratio of less than 1.4. Quadratic 10mm tetrahedral elements were used around the hole of the reference bushing and in the region of the spindle tip, to ensure more accurate results.

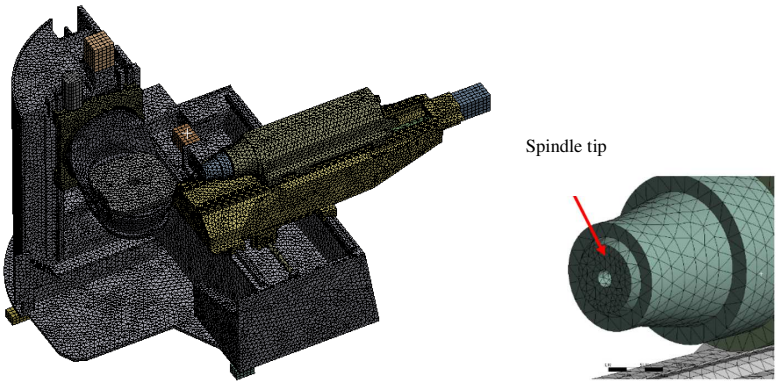

(a) (b)

Figure 4. Finite element mesh of the complete machine (a) and the spindle tip (b).

In the thermoelastic analysis by FEA, the same operational and environmental conditions in which the machining center was exposed during the experimental stage were portrayed, such as speeds of the feed units, periods of machine movement, ambient temperature and heat generation at the critical points of the machine. The thermal errors obtained by FEA were measured by the displacement of the spindle tip (Figure 4b) to 6 positions of each of the three linear axes analyzed.

Experimental error measurements were performed at 33 stop positions of each linear axis of the machine, which represented an error reading every 23 mm. The FEA simulation of these errors will be performed for 6 stops per axis only, due to the time required for each simulation, around 5 hours. This will therefore represent a reading approximately every 150 mm, thus filling the entire length of the travel of each linear axis.

Figure 5 shows the CAD drawing of the machine at some of the defined stopping positions for measuring the thermal error on the X axis. As performed during the experimental steps, the reading of the simulated thermal error was performed after the warm-up cycle ending, considering though the final temperatures obtained, where the machine operated moving all its axes with a linear speed of 30 m/min for a period of 4 hours.

To reach this goal, the CAD model of the machine was designed in 6 different positions. Pos. 1 corresponds to the carriage positioned at coordinate X = 0 mm, Pos. 2 corresponds to coordinate X = 138 mm, Pos. 3 corresponds to X = 299 mm, Pos. 4 corresponds to X = 460 mm, Pos. 5 corresponds to X = 621 mm and Pos. 6 corresponds to X = 759 mm, which is the end of X axis travel. For the machine positioned in each of these intervals of the X axis, was considered the warm-up cycle simulation, where the temperatures in the 15 sensors locations and the error in X of the motor spindle tip were measured.

Figure 5 shows the machine in the X stop positions: 1, 3, 4 and 6.

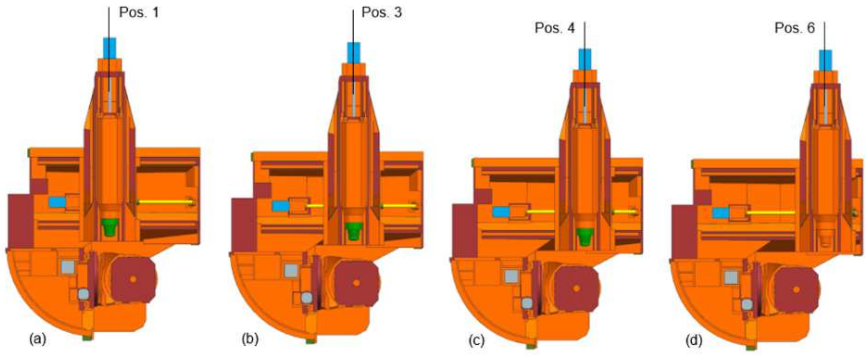

Figure 5. Positioning of the cross carriage for FEA simulation (a) Pos. 1 = 0 mm, (b) Pos. 3 = 299 mm, (c) Pos. 4 = 460 mm, (d) Pos. 6 = 759 mm

Figure 6 shows the CAD drawing of the machine at some of the defined stopping positions for measuring the thermal error of Y-axis positioning. The CAD model of the machine was designed with 6 different positions for the worktable. Pos. 1 corresponds to the work table positioned at Y coordinate = 0 mm, Pos. 2 corresponds to Y coordinate = 162.4 mm, Pos. 3 corresponds to Y = 324.8 mm, Pos. 4 corresponds to Y = 487.2 mm, Pos. 5 corresponds to Y = 696 mm and Pos. 6 is equivalent to Y = 904.8 mm, which is the end of the Y axis travel. For the machine positioned in each of these intervals of the Y axis, the warm-up cycle was simulated, where the temperatures in the 15 sensors and the absolute Y error of the reference bushing located on the worktable were measured. Figure 6 shows the machine CAD at the Y stop positions: 1, 3, 4 and 6.

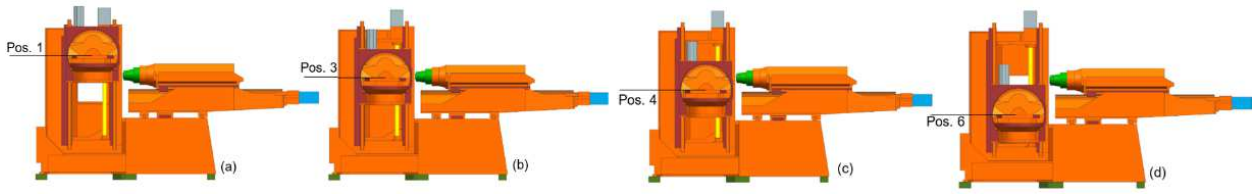

Figure 6. Positioning the worktable for FEA simulation (a) Pos. 1 = 0 mm, (b) Pos. 3 = 324.8 mm, (c) Pos. 4 = 487.2 mm, (d) Pos. 6 = 904.8 mm.

Figure 7 shows the CAD drawing of the machine at some of the defined stopping positions for measuring the thermal error of the Z axis positioning. During this simulation step, the CAD model of the machine was drawn with 6 different positions for the spindle assembly. Pos. 1 corresponds to the spindle positioned at Z coordinate = 0 mm, Pos. 2 corresponds to Z coordinate = 184 mm, Pos. 3 corresponds to Z = 368 mm, Pos. 4 corresponds to Z = 552 mm, a Pos. 5 corresponds to Z = 713 mm and Pos. 6 corresponds to Z = 897 mm, which is the end of the Z axis travel. For the machine positioned in each of these intervals of the Z axis, cycle 4 was simulated, where the temperatures in the 15 sensors and the Z error of the spindle tip were measured. Figure 7 shows the machine in the Z stop positions: 1, 3, 4 and 6.

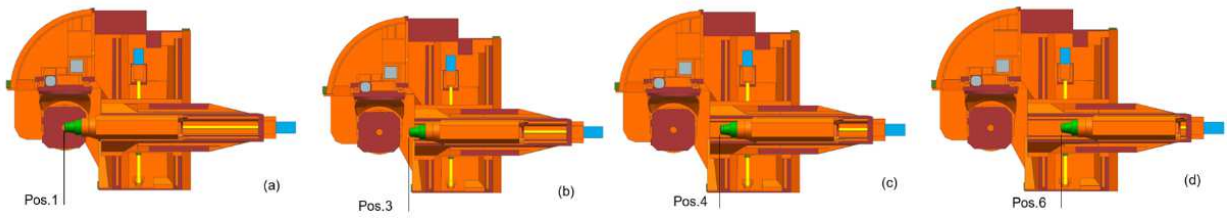

Figure 7. Positioning of the spindle assembly for FEA simulation: (a) Pos. 1 = 0 mm, (b) Pos. 3 = 368 mm, (c) Pos. 4 = 552 mm, (d) Pos. 6 = 897 mm.

3. RESULTS AND DISCUSSIONS

3.1 Experimental measurements

Through laser interferometer, it was possible to measure the positioning thermal errors of the linear axes X, Y and Z of the machining center, as indicated in Figure 8.

Figure 8. Measurement of the positioning of the linear axes (a) Z, and (b) X.

Figure 9 shows the results of temperatures read by the 15 sensors during the performance of the warm-up cycle. This thermal condition of the machine was continuously monitored and used for the measurements of thermal errors in the second stage.

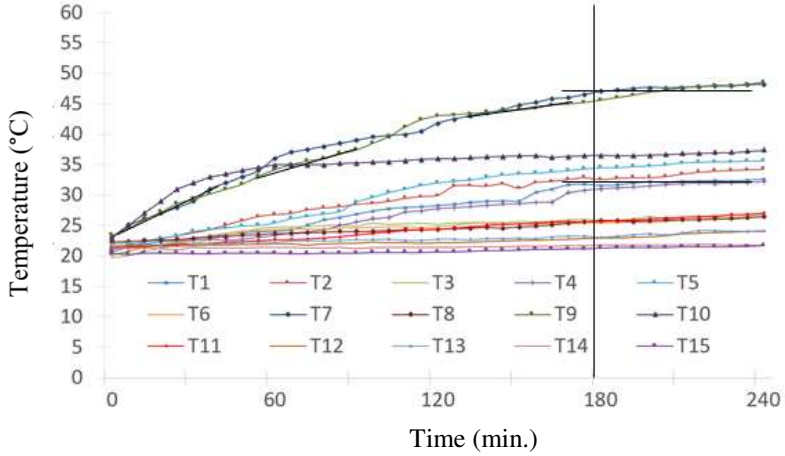

Figure 9. Machine thermal behavior during the warm-up cycle.

In Figure 9, it is observed that the greatest temperature variation occurred for the Y-axis ball screw nut, read by sensor T7, reaching a final temperature of 48.2 °C. Next comes the reading from sensor T9, installed in the Y-axis bearing with a temperature rise of 23.7 °C. The T1 sensor installed on the X-axis ball screw nut reached a maximum temperature of 37.4 °C, while the X-axis bearing, read by T2 had a thermal gradient of 14.5 °C. The Z-axis motor bearing achieved a thermal gradient of 14.1 °C (T5) while the motor spindle achieved 14.4 °C (T10). It can be seen that for most cases, the tendency of thermal stabilization occurs after 3 hours of testing.

The graphs of the relative thermal positioning errors will be presented, that is, the initial geometric positioning errors of the machine, which were obtained in the measurements of the "cold" machine (nominal value), have already been subtracted. This procedure was performed because the objective of this research is to study only the individual contribution of the heating of the subsystems of the X, Y and Z axes in the linear positioning errors of these axes.

The measurement of the thermal error of X axis positioning was performed every 23 mm of the 760 mm X travel, totaling 33 measurements in each thermal condition studied. With 33 measurements in the cold machine condition and 33 measurements in the heated machine condition. The graph in Figure 10 shows the behavior of the X-axis positioning thermal error along the entire travel after the machine warm-up cycle.

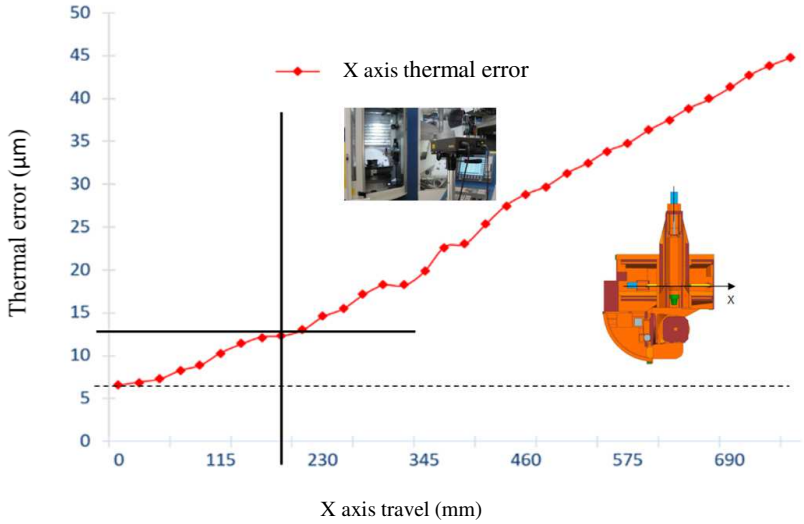

Figure 10. X-axis thermal error obtained by the Laser Interferometer measurement.

At each displacement of the X feed unit by 23 mm, its position was measured, comparing the obtained value with the nominal value. The graph in Figure 6 shows the results of relative thermal errors, already subtracted from the geometric error values, which were computed in the cold machine condition. It is verified that at position X = 0 mm there is already a thermal error of 6.2 µm. It is also observed that in the first intervals of the X axis, between the 0 mm and 150 mm travels, the thermal error variation is small, not exceeding 5.0 µm. This is justified by the reduced length of the ball screw in this section and the restriction to displacements in this direction. From there, there is a practically linear increase in the thermal error in X, reaching 44.8 µm in the 760 mm travel.

The measurement of the thermal error of Y axis positioning was performed every 23.2 mm of the 905 mm Y travel, totaling 39 measurements in each thermal condition studied. With 39 measurements in the cold machine condition and 39 measurements in the heated machine condition. The graph in Figure 11 shows the behavior of the Y-axis positioning thermal error along the entire travel after the heating cycle has been performed. At each displacement of the Y table unit by 23.2 mm, a measurement of its position was performed, comparing the obtained value with the nominal value.

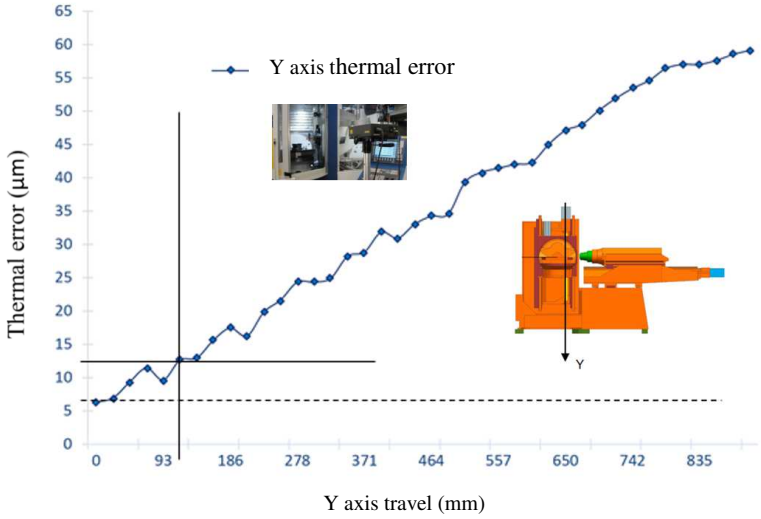

Figure 11. Y-axis thermal error obtained by the Laser Interferometer measurement.

Figure 11 shows the results of relative thermal errors, already subtracted from the geometric error values. Note that at the 0 mm coordinate there is already a thermal error of 7.1 µm. It is also observed that in the first intervals of the Y axis, between the 0 mm and 100 mm travels, the thermal error variation is small, not exceeding 4.0 µm. From then on, there is an almost linear increase in the thermal error in Y, reaching 65.0 µm in the 905 mm travel.

The measurement of the Z axis positioning thermal error was performed every 23 mm of the 897 mm Z travel, totaling 39 measurements in each thermal condition, being 39 measurements in the cold machine condition and other 39 measurements in the heated machine condition. The graph in Figure 12 shows the behavior of the Z axis positioning

thermal error along the entire travel after the machine warm-up cycle. At each displacement of the Z feed unit by 23 mm, a measurement of its position was performed, comparing the obtained value with the nominal value.

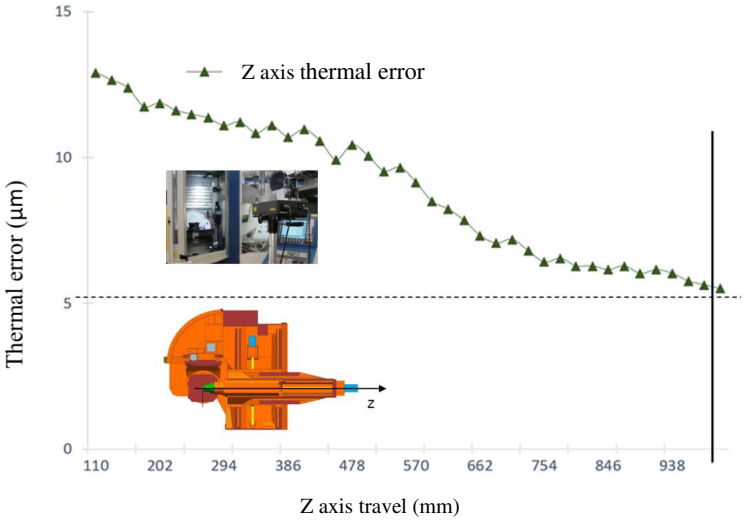

Figure 12. Z-axis thermal error obtained by the Laser Interferometer measurement.

Figure 12 shows the results of relative thermal errors, already subtracted from the geometric error values. It is observed that in the first interval of the measured Z axis, at the Z coordinate = 110 mm, the thermal error is maximum, reaching 12.9 µm. This is justified because the initial position of the Z axis is centered on the worktable, therefore in the largest displacement of the Z axis. From then on, there is a practically linear decrease in the thermal error in Z, reaching 5.5 µm in the travel 938 mm.

3.2 Numerical simulation results

Figure 13 shows the results obtained for each of the 6 positions simulated by FEA in comparison with the errors read experimentally by the laser interferometer at the same positions of the X axis. The simulated thermal errors shown in Figure 13 were measured directly at the spindle tip, thus as performed by the experimental measurement through the laser.

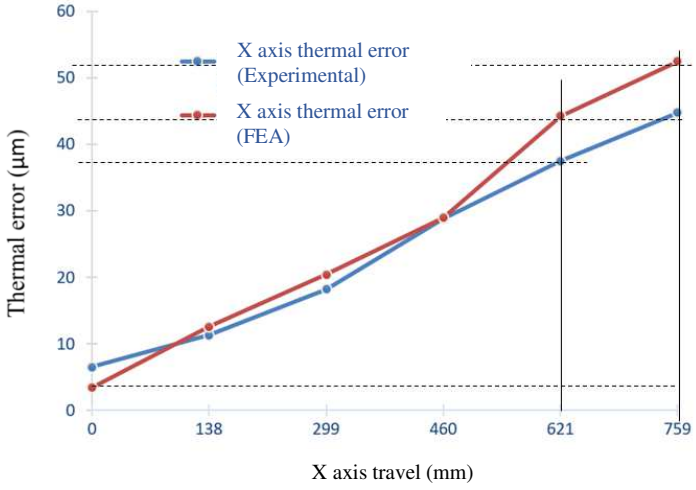

Figure 13. Comparison of thermal error of X-axis positioning experimental by interferometer laser and simulated by FEA.

In Figure 13, there is a difference of 3.1 µm between the experimental measurement and FEA at the initial position of the X travel. This is due to the difficulty in modeling the heat generated in the region of the coupling of the ball screw shaft with the motor in that region. The relative error decreases, reaching differences below 1.0 µm, as in the positions 138 mm and 460 mm. In the 621 mm and 759 mm stretches of the X travel, there was an increase in the difference between the measured values of 6.7 µm and 7.5 µm, respectively. This difference is attributed to the degree of complexity of the

heat model generated in this region. Anyway, for purposes of volumetric thermal error modeling, it is considered that the individual thermal error behavior in X was simulated satisfactorily.

Figure 14 shows the results obtained for each of the 6 positions simulated by FEA in comparison with the errors read by the interferometer laser at the same Y axis positions. The simulated thermal errors shown in Figure 14 were measured directly on the reference bushing.

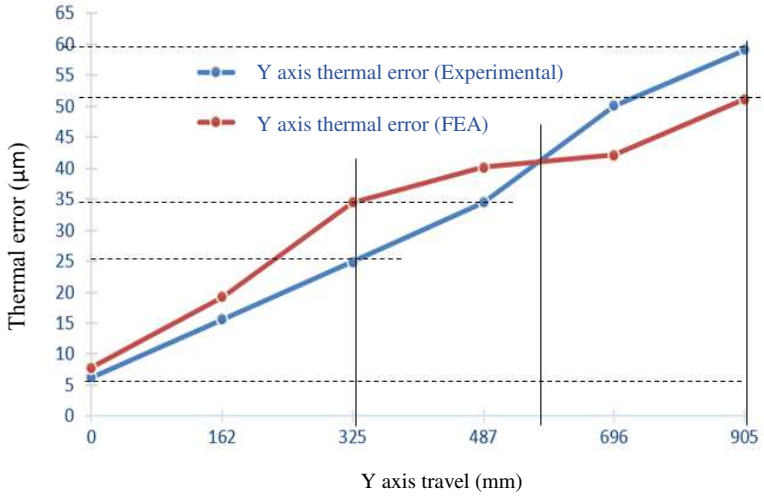

Figure 14. Comparison of the thermal error of Y-positioning experimental by interferometer laser and simulated by FEA.

In Figure 14, there is a difference of 1.5 µm between the experimental measurement and MEF at the initial position of the Y travel. The experimental thermal error at this position was 6.3 µm while the simulated error was 7.8 µm. From this stretch onwards, the relative error increases slightly, reaching differences of 9.6 µm at 324.8 mm and 5.6 µm at 487.2 mm. In the 696 mm and 904.8 mm sections of the Y travel, the difference between the simulated and measured values stabilizes at 8.0 µm. Again, this average difference in the order of 6.0 µm is attributed to the degree of complexity of the heat generation model in the region. For the purpose of volumetric modeling of thermal error, it is considered that the behavior of the thermal error individually in Y has been satisfactorily simulated.

Figure 15 shows the results obtained for each of the 6 positions simulated by FEA in comparison with the errors read by the interferometer laser in the same positions of the Z axis. The simulated thermal errors shown in Figure 15 were measured directly at the spindle tip, as well as performed by experimental measurement.

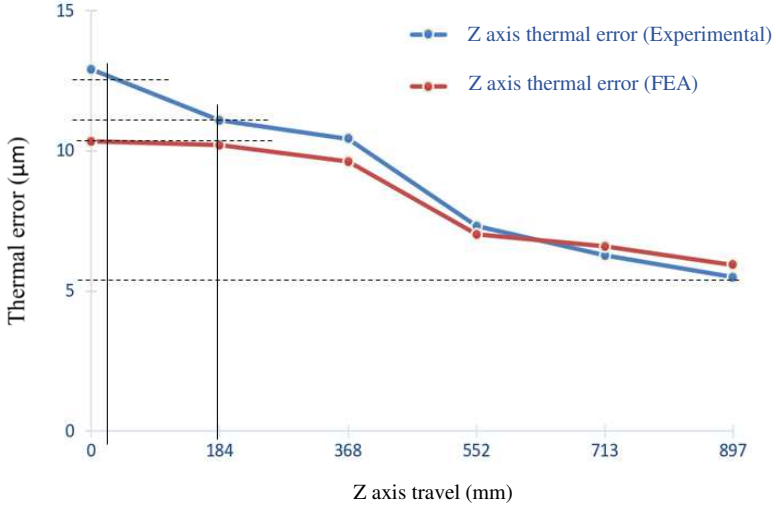

Figure 15. Comparison of the thermal error of Z positioning experimental by interferometer laser and simulated by FEA.

In Figure 15, there is a difference of 2.5 µm between the experimental measurement and FEA in the initial position of the Z travel, which corresponds to the most advanced travel of the pin, aligned with the center of the table. The

experimental thermal error at this position was 12.9 µm while the simulated error was 10.4 µm. From this stretch on, the relative error decreases, reaching differences of less than 1.0 µm, in addition to the same thermal error behavior trend for all other analyzed stretches. Including the most indented position of the Z axis, at coordinate 897 mm, which was more critical on the other axes. For purposes of volumetric thermal error modeling, it is considered that the individual thermal error behavior in Z was also simulated satisfactorily.

4. CONCLUSIONS

After carrying out this research, whose main objective was to reproduce the thermal errors that occur in the machining center through numerical simulation, it was possible to conclude that:

- A strategic advantage of using laser interferometer measurements to meet the objectives of this research, is the fact that it allows the individualization of thermal positioning errors for each linear axis.
- The MEF simulation of the laser measurement of the positioning of the linear axes X, Y and Z of the machining center proved to be satisfactory, since the main contribution of this work was to be able to reproduce the same thermal errors obtained by the real operation of the machine through numerical simulation.
- The difference between the values obtained experimentally and those simulated was less than 10 µm in all simulated cases. Most errors were between 4 µm and 6 µm.
- It is attributed to the fact that greater differences are obtained in the modeling of the Y axis due to the greater complexity of this machine subsystem, which involved heating the ball screw, linear guides and also the rotary tables of the machine.

5. ACKNOWLEDGEMENTS

The authors would like to acknowledge the companies B. GROB of Brazil and ESSS - ANSYS for their support in providing equipment and software.

6. REFERENCES

Abdulshahed, A.M., Longstaff, A.P., and Fletcher, S., 2015. “The Application of ANFIS Prediction Models for Thermal Error Compensation on CNC Machine Tools”. Applied Soft Computing Journal, Vol. 27, pp. 158–68.

Drossel, W.G., Ihllenfeldt, S.T., and Zwingerberger, C., 2013. “Modellierung des Wärmeaustauschs Maschine-Umgebung”. 16. Dresdner Werkzeugmaschinen-Fachseminar – Fraunhofer IWU Chemnitz, pp. 95 – 113.

Gurauskis, D., Kilikevičius, A., Borodinas, S., and Kasparaitis, A., 2019. “Analysis of geometric and thermal errors of linear encoder for real-time compensation”. Sensors and Actuators A: Physical, Vol. 296, pp. 145–154.

Jedrzejewski, J., Kwasny, W., Kowal, Z., and Modrzycki, W., 2008. “Precise Model of HSC Machining Centre for Aerospace Parts Milling”. Journal of Mechanical Engineering Vol. 8, No 3, pp. 29–41.

Liu, C., Vengayil, H., Zhong, R.Y., and Xu, X, 2018. “A systematic development method for cyber-physical machine tools”. Journal of Manufacturing Systems. Vol. 638, pp. 38-51.

Liu, J., Ma, C., Gui, H., and Wang, S., 2021. “Thermally-Induced Error Compensation of Spindle System Based on Long Short Term Memory Neural Networks”. Applied Soft Computing, Vol.102. pp. 42-58.

Liu, T., Gao, W., Zhang, D., Zhang, Y., Chang, W., and Liang, C, 2017. “Analytical Modeling for Thermal Errors of Motorized Spindle Unit”. International Journal of Machine Tools and Manufacture, Vol. 112, pp. 53–70.

Mayr, J., Jedrzejewski, J., Uhlmann, E., Donmez, M.A., Knapp, W., Härtig, F., Wendt, K., and Wegener, K., 2012. “Thermal issues in machine tools”. CIRP Annals - Manufacturing Technology, Vol. 61, No 2, pp. 771-791.

Miao, E., Liu, Y., Liu, H., Gao, Z., and Li, W., 2015. “Study on the effects of changes in temperature-sensitive points on thermal error compensation model for CNC machine tool”. International Journal of Machine Tools and Manufacture, Vol. 97, pp. 50-59.

Zhang, B., and Wu, J., 2019. “Modeling and optimizing”. Journal of Engineering Manufacture, Vol. 52, pp. 1-14.

Zhao, D., Bi, Y., and Ke, Y., 2017. “An efficient error compensation method for coordinated CNC five-axis machine tools”. International Journal of Machine Tools and Manufacture. Vol. 123, pp. 105-115.

Zhou, H., Hu, P., Tan, H., Chen, J., and Liu, G., 2018. “Modelling and compensation of thermal deformation for machine tool based on the real-time data of the CNC system”. Procedia Manufacturing. Vol. 26, pp. 1137-1146.

7. RESPONSIBILITY NOTICE

The authors are the only responsible for the printed material included in this paper.